International Journal of Smart Home
Vol. 9, No. 10, (2015), pp. 107-116
http://dx.doi.org/10.14257/ijsh.2015.9.10.12

# Analysis of Impact of Terrain Factors on Landscape-scale Solar Radiation

Xiaodan Mei[1, 2], Wenyi Fan[1] and Xuegang Mao[1]

[1] *School of Forestry, Northeast Forestry University, Harbin150040, China*
[2] *Schools of Surveying and Mapping Engineering, Heilongjiang Institute of Technology, Harbin150050, China*
*E-mail:mxd2014ch@163.com*

***Abstract***

*Incident solar radiation is one of the major sources of energy for driving biological and physical processes on earth. In this paper, simple conversion factors are designed to determine how the four landforms (i.e. plain, plateau, hill and mountain) will affect incident solar radiation at one month intervals using the ArcGIS tool appropriate for regional solar radiation analysis. A comparison is made between simulation results and those measurements taken in actual radiation stations, providing a correlation $R^2$ of 0.9063. Results indicate first, that if the ratio of the monthly mean of the DEM-based regional solar radiation to the monthly mean of the hypothesis DEM-based regional solar radiation is defined as the conversion factor (R) of the solar radiation and the ArcGIS tool for regional solar radiation analysis is employed, then the computation can be simplified and the impact of terrain factors on incident solar radiation can be correctly represented. Secondly, with each of the four landforms, R varies according to the season, slope gradient and aspect; the season induces more impacts than the terrain factors; R increases first and then decreases when the aspect changes clockwise, but decreases continuously with an increase in slope grade; R varies in a complex way in the case of mountains, especially for grade-five slopes. Thirdly, R increases initially and then decreases in a sinusoidal manner with an increase in aspect under the influence of slope gradient during the winter; R varies in a linear and somewhat symmetric manner (monotone increasing, monotone decreasing and stable) with the increase in slope gradient and under the influence of the aspect. These results are helpful in studying the impact of terrain factors of different landforms on incident solar radiation on the landscape scale using the simple conversion factors.*

***Keywords:*** *terrain factors, incident solar radiation, landscape scale, ArcGIS, landforms*

## 1. Introduction

On the landscape scale, terrain is a predominant factor which determines spatial-heterogeneity incident solar radiation. Considerable research has been carried out around the world theoretically and technically in order to compute solar radiation in fluctuating terrains using GIS [1-6], and these results have been used widely [7-12]. However, in previous studies, the ratio of astronomical radiation for fluctuating terrains to astronomical radiation for horizontal planes is defined as the conversion factor, and computed via the formula and solar radiation calculation model. The impact of local terrain factors on solar radiation [13-18] have also been considered, resulting in heavy computational loads. Furthermore, these works are not universal, thus leading to the spatial resolution based on DEM grid data being too low [18-20]. In addition, characteristic points of landforms are usually selected as sampling points [13-20]; and grid units of specific altitudes, slope gradients and aspects are selected manually. All

ISSN: 1975-4094 IJSH

these factors therefore make each selection process too unique and prone to being confounded by anthropic factors. In this paper, simple conversion factors are designed on the landscape scale based on 30m*30m GDEM data by means of the ArcGIS tool for regional solar radiation analysis; the landforms are categorized into plain, plateau, hill or mountain according to the altitude and degree of terrain fluctuation; and the impact of terrain factors of different landforms on incident solar radiation is analyzed.

## 2. Research Area and Method

### 2.1. Overview of Research Area

Jiamusi is located in the northeast of Heilongjiang, with a north latitude of 45°56′ ~ 48°28′ and east longitude of 129°29′ ~ 135°5′, covering an area of 327,000 $km^2$. The city has a temperate, continental, monsoon climate, which often has rain and high temperatures occurring at the same time. Its landform varies between its mountain, hill and plain from the southwest to northeast where the altitude is low. In this paper, we focus on the Jiamusi region to analyze ArcGIS-based regional solar radiation in different landforms.

### 2.2. Data Preparation

(1) Vector data: The Jiamusi radiation station has a latitude of 46°49′N and a longitude of 130°17′E. Based on its location, ArcGIS is used to generate the point vector elements (*.shp). The coordinate system is WGS-84, the projection type is UTM Zone 52N, and the data format is Shapefile (*.shp);

(2) Radiation data: The daily datasets from the Jiamusi radiation station and the ground climate station are derived from China's meteorological data sharing service website (http://cdc.cma.gov.cn/home.do). The daily value of solar radiation at the Jiamusi radiation station in 2012, *i.e.* daily radiant exposure (0.01 $MJ/m^2$), was extracted from the daily dataset of the research area; and the monthly sum of the daily radiant exposure from the period January to December was computed as the monthly mean of incident solar radiation;

(3) Terrain data: the GDEM digital elevation information of the Jiamusi region is derived at a resolution of 30 m from the mirror site of the international scientific data, Computer Network Information Center, Chinese Academy of Science (http://www.gscloud.cn). Its projection type is UTM/WGS84, its spatial resolution is 30 m, and the data format is ImageFile (*.img).

To further analyze the impact of terrain factors of different landforms on incident solar radiation with fluctuating terrains, we classify the research area into different landforms according to the altitude and terrain fluctuation degree computed by DEM. The ArcGIS tool for neighborhood analysis and DEM are used to compute the terrain fluctuation degree (or relief) of the research area. Experiments are performed through different analysis windows (3*3-50*50) of the terrain fluctuation degree. Based on the plot describing terrain fluctuation degree of the research area, 35*35 is chosen as the optimal analysis window of the research area, because it has an obvious inflection point which subsequently achieves stability. The research area is classified into different landforms according to the characteristics of terrains in our country, charting regulations, plains (<30m), plateaus (30m ~ 70m), hills (70 ~ 200m) and mountains (>200m), as well as altitudes and terrain fluctuation degrees.

 

### 2.3. Research Method

Only earth movement and terrain is taken into account in order to eliminate the effect of other extraneous factors on incident solar radiation. Traditionally, the ratio of astronomical radiation in the fluctuating terrains to the astronomical radiation in the horizontal plane is defined as the conversion factor. However, for the purposes of this paper, the ratio of monthly mean of the DEM-based regional solar radiation to the monthly mean of the hypothesis DEM-based regional solar radiation, is defined as the conversion factor (R). In the hypothesis DEM, the grid computation method is used to set the DEM of the entire research area to zero, assuming this is a flat area independent of slope gradient and direction. Therefore, R is helpful in amplifying the impact of terrain fluctuation on incident solar radiation and thereby eliminating the effect of other factors. The ArcGIS tool for regional solar radiation analysis was employed to simulate the monthly quantity (sum of the daily)of incident solar radiation throughout 2012. By computing R by the ratio of field calculation, variations of R, according to the season, slope gradient and direction indifferent landforms and throughout the entire area, are analyzed. In ArcGIS analysis of solar radiation, the reflected radiation is neglected, such that the total quantity of solar radiation is equal to the sum of direct radiation and scattered radiation. The solar radiation analysis tool is used as the chosen method for computing the incident solar radiation in a particular landscape or at a certain location. This method was developed by Rich at al., based on the hemispheric view shed algorithm [21-22] and further improved by Fu [23-25]. Terrain and radiation parameters are set up by default in the simulations. To adequately represent the relation between solar radiation and terrain factors across the region, terrain factors analysis are performed on the grid units of all solar radiation simulation results in the research area. Owing to the large amount of data, R is the average of all grid points classified into different landforms, aspects and gradients. Furthermore, ArcGIS analysis of solar radiation is conducted on the landscape scale and local scale, so the average latitude for the research area automatically computed by DEM is used as the latitude, which is equal to 46.69°N. The simulation result (in W/m2) is compared with the actual measurements provided by the radiation station for verification and analysis in Figure 1.

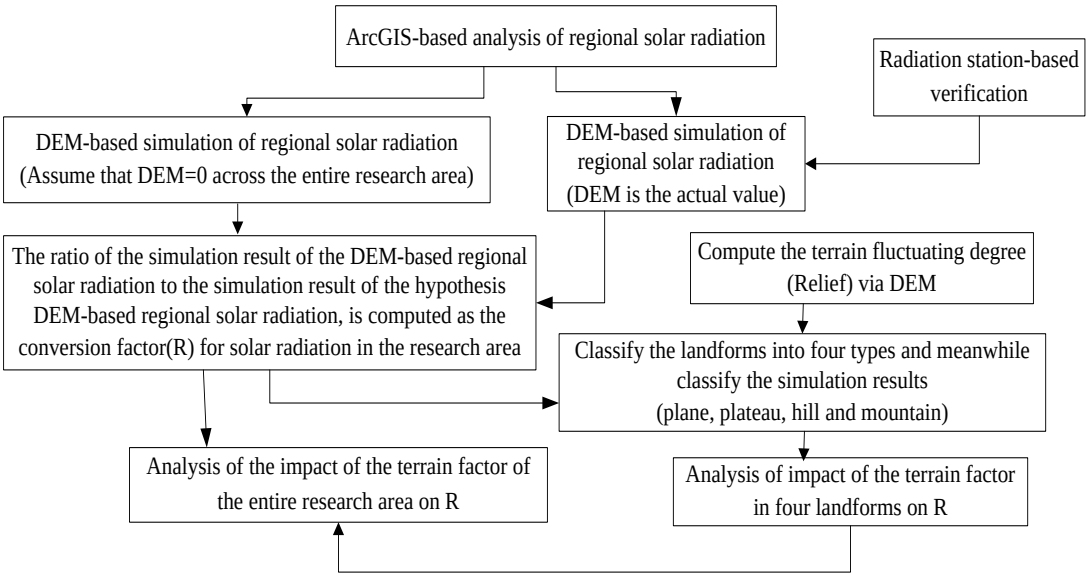


**Figure 1. ArcGIS-Based Simulation of Regional Solar Radiation**

# 3. Result and Analysis

## 3.1. Verification and Analysis of Simulation Results

The hypothesis DEM-based regional solar radiation simulation result and the DEM-based regional solar radiation simulation result are both the monthly mean of all grid units across the region. The results in Table 1 show that when the DEM values are zero throughout the region, *i.e.* the altitude of this region is 0 m, the region can be regarded as flat. In this case, the monthly value ($W/m^2$) of incident solar radiation in each grid unit throughout 2012 is constant and equal to each other. Nevertheless, the simulation result still demonstrates the impact of season on incident solar radiation. With other factors remaining equal, the DEM-based regional solar radiation simulation result becomes more complex under the influence of slope gradient, aspect and terrain factors, and therefore its monthly mean is greater than the hypothesis DEM-based simulation result. However, the ordering of seasons represented by a month is the same in both cases: July (summer) >April (spring) >October (autumn) >January (winter).

**Table 1. Comparison of Simulation Results of Hypothesis DEM-base and DEM-Based Regional Solar Radiation ($W/m^2$)**

| | Jan. | Feb. | Mar. | Apr. | May | Jun. | Jul. | Aug. | Sep. | Oct. | Nov. | Dec. |
|---|---|---|---|---|---|---|---|---|---|---|---|---|
| hypothesis-based DEM | 16271 | 32726 | 74943 | 117167 | 158538 | 168016 | 165975 | 134353 | 88037 | 44103 | 19099 | 11645 |
| DEM-based | 16450 | 32959 | 75320 | 117719 | 159342 | 168916 | 166839 | 134996 | 88462 | 44381 | 19288 | 11795 |

The monthly values achieved in the simulation are compared with those computed using solar radiation measurements from the Jiamusi radiation station. Correlation analysis is performed on both the simulated value and measured value. Results in Figure 2 show that the correlation ($R^2$) between the simulated value and the measured value for the total quantity of ArcGIS incident solar radiation throughout the year is 0.9063. This demonstrates that it is feasible to simulate the monthly value of incident solar radiation using ArcGIS regional solar radiation to a high degree of accuracy.

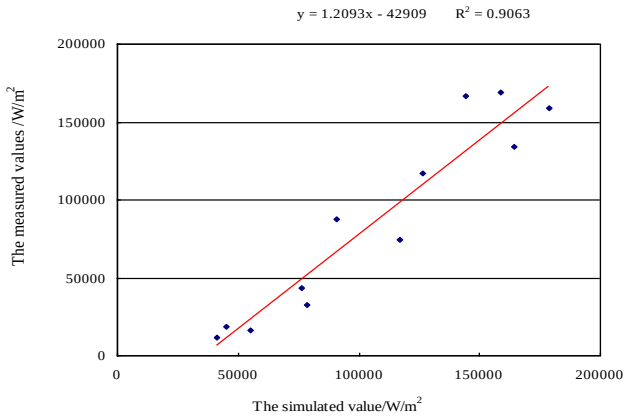


**Figure 2. Correlation between Simulated Value and Measured Value**

## 3.2. Variation of R with Season, Slope Gradient and Direction in Different Landforms

Measurement is performed in a clockwise rotation beginning with due north for aspect. Omitting flat areas, 8 default aspects in ArcGIS are used here: North（0°~22.5°）and （337.5°~360°）, Northeast（22.5°~67.5°）, East（67.5°~112.5°）, Southeast（

112.5°~157.5°), South (157.5°~202.5°), Southwest (202.5°~247.5°), West (247.5°~292.5°) and Northwest (292.5°~337.5°). The slope gradient is defined based on Technical Regulation on the Second National Land Survey of China: grade 1 (0°~2°), grade 2 (2°~6°), grade 3 (6°~15°), grade 4 (15°~25°), and grade 5 (>25°). Variations of R with seasons in four different landforms are given in Table 2. Results show that R varies according to season in the four variants of landform. When the aspect changes clockwise, R initially increases and then decreases in January, April, July and October; R is higher for the south slope and lower for the north slope, and can be seen to vary most radically in January with aspect. In other words, the aspect has a greater impact on R in winter. Based on the variation ranges and peak values of R, the landforms can be sorted as mountain > hill >plateau> plain. Variations of R with slope gradient in four landforms are shown in Table 3. Results show that R varies similarly with slope gradient in the landforms of plateau and hill, decreasing with an increase in slope gradient during different seasons; that is, grade-1 provides the largest value of R while grade-5 provides the lowest; and R decreases most radically with increases in slope gradient in the plateau, but changes slightly in the hill. For plains without five grades of slope, R remains stable across slope gradients during the different seasons. In the case of the mountain, R changes in a complex fashion. It varies proportionately with slope gradient from grade 1 to 4 during the different seasons, decreasing with an increase in slope gradient. However, for grade-5 slopes, R increases along with slope gradient in January, April and October. R varies most radically with slope gradient in January; that is, slope gradient has the greatest impact on R in winter. Based on the variation range of R, the landforms can be sorted as plateau > mountain > hill > plain.

**Table 2. Variation of R with Aspect in Different Landforms**

| Aspect (°) | Plane | | | | Plateau | | | | Hill | | | | Mountain | | | |
|---|---|---|---|---|---|---|---|---|---|---|---|---|---|---|---|---|
| | month | | | | | | | | | | | | | | | |
| | 1 | 4 | 7 | 10 | 1 | 4 | 7 | 10 | 1 | 4 | 7 | 10 | 1 | 4 | 7 | 10 |
| North (0°~22.5°) | 0.91 | 0.97 | 0.99 | 0.94 | 0.80 | 0.93 | 0.96 | 0.86 | 0.80 | 0.94 | 0.97 | 0.86 | 0.80 | 0.94 | 0.97 | 0.86 |
| Northeast (22.5°~67.5°) | 0.94 | 0.98 | 0.99 | 0.96 | 0.80 | 0.91 | 0.94 | 0.85 | 0.79 | 0.91 | 0.94 | 0.84 | 0.81 | 0.93 | 0.96 | 0.86 |
| East (67.5°~112.5°) | 1.02 | 1.01 | 1.01 | 1.01 | 0.98 | 0.97 | 0.97 | 0.97 | 1.00 | 0.98 | 0.98 | 0.99 | 0.99 | 0.99 | 0.99 | 0.98 |
| Southeast (112.5°~157.5°) | 1.09 | 1.03 | 1.02 | 1.06 | 1.16 | 1.03 | 1.00 | 1.10 | 1.25 | 1.06 | 1.02 | 1.16 | 1.31 | 1.08 | 1.04 | 1.20 |
| South (157.5°~202.5°) | 1.12 | 1.04 | 1.02 | 1.08 | 1.21 | 1.06 | 1.03 | 1.15 | 1.35 | 1.10 | 1.04 | 1.23 | 1.38 | 1.11 | 1.05 | 1.25 |
| Southwest (202.5°~247.5°) | 1.09 | 1.03 | 1.02 | 1.06 | 1.20 | 1.05 | 1.02 | 1.13 | 1.24 | 1.06 | 1.02 | 1.16 | 1.32 | 1.09 | 1.04 | 1.21 |
| West (247.5°~292.5°) | 1.01 | 0.99 | 0.99 | 1.00 | 0.96 | 0.97 | 0.97 | 0.96 | 0.99 | 0.98 | 0.98 | 0.98 | 0.98 | 0.98 | 0.99 | 0.98 |
| Northwest (292.5°~337.5°) | 0.89 | 0.96 | 0.97 | 0.92 | 0.79 | 0.91 | 0.95 | 0.84 | 0.80 | 0.91 | 0.94 | 0.84 | 0.81 | 0.93 | 0.96 | 0.85 |
| North (337.5°~360°) | 0.91 | 0.97 | 0.99 | 0.94 | 0.81 | 0.93 | 0.97 | 0.86 | 0.71 | 0.86 | 0.91 | 0.75 | 0.72 | 0.89 | 0.94 | 0.78 |

**Table 3. Variation of R with Slope Gradient in Different Landform**

| Slope (°) | Plane | | | | Plateau | | | | Hill | | | | Mountain | | | |
|---|---|---|---|---|---|---|---|---|---|---|---|---|---|---|---|---|
| | month | | | | | | | | | | | | | | | |
| | 1 | 4 | 7 | 10 | 1 | 4 | 7 | 10 | 1 | 4 | 7 | 10 | 1 | 4 | 7 | 10 |
| grade 1 (0°~2°) | 1.016 | 1.008 | 1.007 | 1.011 | 1.018 | 1.009 | 1.008 | 1.013 | 1.025 | 1.012 | 1.011 | 1.017 | 1.035 | 1.019 | 1.018 | 1.026 |
| grade 2 (2°~6°) | 1.013 | 1.006 | 1.005 | 1.009 | 1.011 | 1.006 | 1.006 | 1.007 | 1.018 | 1.010 | 1.011 | 1.012 | 1.024 | 1.015 | 1.016 | 1.017 |
| grade 3 (6°~15°) | 0.997 | 0.996 | 0.997 | 0.996 | 1.010 | 1.001 | 1.000 | 1.004 | 1.001 | 0.999 | 1.002 | 0.997 | 0.961 | 0.988 | 0.998 | 0.970 |
| grade 4 (15°~25°) | 0.970 | 0.963 | 0.961 | 0.967 | 0.976 | 0.964 | 0.964 | 0.969 | 1.017 | 0.984 | 0.982 | 0.997 | 0.950 | 0.964 | 0.973 | 0.950 |
| grade 5 (>25°) | non-value | | | | 0.718 | 0.834 | 0.864 | 0.766 | 0.977 | 0.905 | 0.897 | 0.936 | 1.115 | 0.969 | 0.951 | 1.026 |

### 3.3. Variation of R with Season, Aspect and Gradient across the Region

In summary, R varies most radically with season, aspect and gradient in the four landforms during the month of January. Taking this into account, further analysis is performed on variations of R with aspect and gradient across the entire region during January. Variations of R with season, aspect and gradient across the region are plotted, based on computations of R. Variations of R with aspect in January, April, July and October at a slope of grade 4 (15°~25°) are shown in Figure3a. Results show that depending on the aspect, R varies mostly radically in January (winter), followed immediately by October (autumn), and then April (spring) and July (summer). It can be concluded therefore that the impact of aspect on the quantity of incident solar radiation varies according to season. The evident variation in January is similar to that which occurs in October, larger than 1 for the south slope. However, the opposite is apparent in the case of the northern slope. In other words, the quantity of incident solar radiation gained at the south slope is far more intense than that on flat ground, while the magnitude measured at the north one is much less significant. R varies slightly with aspect in April and July, being close to 1. In other words, for the given slope gradient, the quantity of incident solar radiation is almost irrespective of aspect, because the amount of radiation at the slope is almost equal to that on flat ground. Intersections of curves show R approximates to 1 for east and west slopes during the different seasons, i.e. almost the exact same amount of solar radiation acquired throughout the year on these slopes is found to that on flat ground. Because R varies most radically with aspect in January, we opt to further analyze variations of R with aspect and gradient in this particular month. Variations of slope gradient in January are plotted in Figure3b. Results indicate that the impact of slope gradient on R increases with the degree of slope gradient. Hence, the impact of slope gradient can be sorted as: grade-5 > grade-4>grade 3 > grade-2 > grade-1, where R varies radically at slopes of grades 3, 4 and 5, and is close to 1 at slopes of grades 1 and 2.Intersections of curves demonstrate that R is close to 1 at eastern and western slopes with varying grades in winter; specifically, the obtained quantity of incident solar radiation is almost equal to that on flat ground. Variations of R with slope gradient along different aspects in January are shown in Figure 3c. Results highlight that as slope gradient increases, the impact of aspect on R can be determined as south slope > southeast and southwest slope > east and west slope > northeast and northwest slope> north slope; and R varies in three linear manners (monotone decreasing, monotone increasing and stable) along different aspects and also exhibits symmetry. In the case of south, southeast and southwest slopes, R increases gradually and is larger than 1, signifying that the quantity of incident solar radiation at the slope is larger than that on flat ground; for east and west slopes, R is steadily approaching 1, inferring that the amount of incident solar radiation at the slope is almost equal to that on flat ground; at the

 

north, northeast and northwestern slopes, R decreases gradually and is less than 1, indicating that the total quantity of incident solar radiation at the slope is less than that on flat ground. Variations of R at the southeast (northeast) slope are similar to that at the southwest (northwest) slopes. In other words, regions with the same slope gradient at the same latitude in the northern hemisphere, experience almost the same quantity of incident solar radiation.

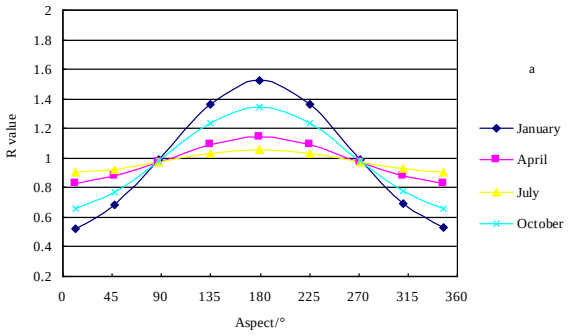


**a. Impact of Aspect on R during Different Seasons**

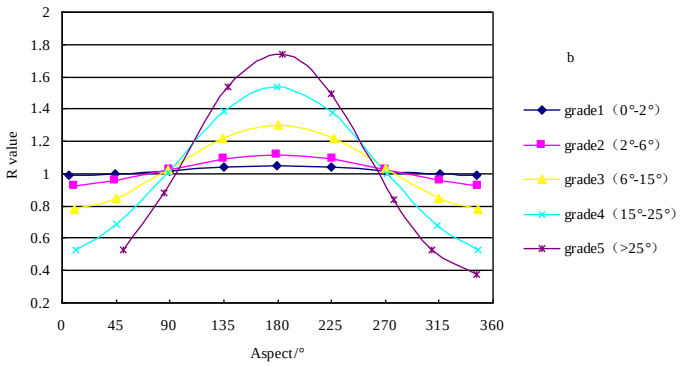


**b. Impact of Aspect on R with Varying Slope Gradients**

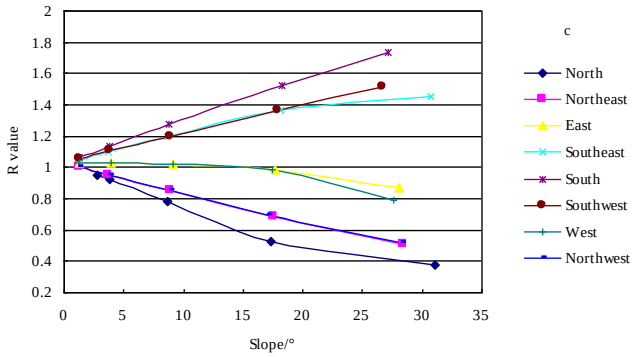


**c. Impact of Slope Gradient on R along Different Aspects**

**Figure 3. Impact of Terrain Factors on R**

## 4. Discussion and Conclusion

(1) We conduct a study of the hypothesis-based DEM and DEM-based simulation of regional solar radiation, compute the ratio (R) of monthly means of their simulation values, and analyze the impact of terrain factors in four landforms on solar radiation. It is found that the season has a significant effect on incident solar radiation on flat ground terrain. During the same season, the slope plays a more notable role in incident solar

radiation than that evidenced on flat ground. The impact of aspect on the amount of incident solar radiation varies according to season; R varies similarly with aspect in four landforms, increasing first and then decreasing; R decreases continuously with slope gradient with an exception of the grade-5 slope where R increases in the mountain during January, April and October. In winter when R varies most discernibly, R fluctuates in a sinusoidal manner (initially increasing and then decreasing) with an increase in aspect for varying slope gradients across the entire region; it monotonically increases, decreases or remains stable based on the increase in slope gradient along different directions, and the variation in different directions is somewhat symmetrical.

(2) To eliminate the impact of other factors on incident solar radiation, we limit our focus on earth movement and terrain. As opposed to previous research using the traditional method, we compute the ratio of monthly means of the DEM-based and the hypothesis DEM-based regional incident solar radiation, and define it as the conversion factor of incident solar radiation. In this way, we can reduce computational loads and more effectively represent the impact of terrain factors on incident solar radiation in different landforms. Furthermore, the study follows the assumption that the impact of terrain on astronomical radiation is consistent with the impact of terrain on direct solar radiation. Therefore it is more suited for sunny weather or the case where scattered radiation accounts for a small proportion of the total quantity of incident solar radiation. In the case of cloudy weather, the ratio of the monthly simulation values of direct solar radiation should be defined as R.

(3) In previous literature, grid units with particular altitudes, aspects and gradients are chosen to study the impact of terrain factors on incident solar radiation. It has also been ascertained that solar radiation on the plateau varies according to season, slope gradient and aspect [16-18]. In this paper however, we rely on GDEM elevation data with a resolution of 30 m, choose all grid units within the region as the mesh point, classify landforms according to slope gradient and altitude, and compute the amount of incident solar radiation as the mean of all mesh points under exactly the same conditions. Therefore, our computation results are universal and can better represent the impact of terrain factors in four landforms across the entire research area on incident solar radiation.

(4) The simulation and verification is flawed as it relies on merely one radiation station within the research region. Future work will require the remote sensing data to be collected over a longer duration. Similarly, further investigation should be conducted on the impact of terrain factor on incident solar radiation at different time scales, and on the verification of solar radiation simulation results at the landscape scale through the use of data fusion techniques.

## Acknowledgments

Helpful review comments were provided by the reviewer. The data were provided by the China meteorological science data sharing service (http://cdc.cma.gov.cn/home.do). This research was funded under Heilongjiang Province Ordinary University key Laboratory of Spatial Geographic Information Comprehensive Laboratory Open Projects (No.KJKF-12-04) and "Twelfth five-year" National Science and Technology Support Project(No. 2011BAD08B01) grants.

## References

[1] Z. Gao, Y. Tian, J. Chen and H. Chen, “A GIS-based study of monthly average global solar radiation”, International Conference on Geoinformatics, vol. 12, no. 9, **(2013)**, pp. 1- 4.
[2] R. Li, X. Liu and Y. Sun, “Integrated Assessment Model for Solar Energy Resource Based on GIS. Multimedia Technology (ICMT)”, 2010 International Conference on IEEE, **(2010)**, pp. 1 - 4.
[3] R. D. Rich and M. Paul, “Topographic solar radiation models for GIS”, International Journal of Geographical Information Systems, vol. 9, no. 4, **(2007)**, pp. 405-419.

 

[4] M. Luoto and M. Seppälä, "Modelling the distribution of palsas in Finnish Lapland with logistic regression and GIS", Permafrost & Periglacial Processes, vol. 13, no. 1, **(2002)**, pp. 17–28.
[5] H. L. He, G. R. Yu and D. Niu, "Method of global solar radiation calculation on complex territories", Resources Science, vol. 25, no. 1, **(2003)**, pp. 78-85.
[6] Y. Zeng, X. F. Qiu and S. M. Liu, "Distributed modeling of extraterrestrial solar radiation over rugged terrains", Chinese Journal of Geophysics, vol. l48, no. 5, **(2005)**, pp. 1028-1033.
[7] X. Jin and L. X. Yang, "Solar radiation calculation under complex topography based on ArcGIS", Anhui Agricultural Sciences, vol. 4, no, 23, **(2014)**, pp. 7952-7955.
[8] M. Migliavacca, E. Cremonese, R. Colombo, L. Busetto, M. Galvagno, L. Ganis and M. Meroni, "European larch phenology in the Alps, can we grasp the role of ecological factors by combining field observations and inverse modeling", International Journal of Biometeorology, vol. 52, no. 7, **(2008)**, pp. 587-605.
[9] C. A. Gueymard, "Clear-sky irradiance predictions for solar resource mapping and large-scale applications", Improved validation methodology and detailed performance analysis of 18 broadband radiative models. Solar Energy, vol. 86, no. 8, **(2012)**, pp. 2145-2169.
[10] H. Alsamamra, J. A. Ruiz-Arias, D. Pozo-Vázquez and J. Tovar-Pescador, "A comparative study of ordinary and residual kriging techniques for mapping global solar radiation over southern Spain", Agricultural & Forest Meteorology, vol. 149, no. 8, **(2009)**, pp. 1343-1357.
[11] M. Rylatt, S. Gadsden and K. Lomas, "GIS-based decision support for solar energy planning in urban environments", Computers Environment & Urban Systems, vol. 25, no. 6, **(2001)**, pp. 579-603.
[12] Z. Q. Chen and J. F. Chen, "The Simulation of Extraterrestrial Solar Radiation Based on DEM in Zhangpu Sample Plot and Fujian Province", Education Technology and Training & Geoscience and Remote Sensing IEEE, **(2008)**, pp. 551-554.
[13] J. Tovar-Pescador , D. Pozo-Vázquez , J. A. Ruiz-Arias, J. Batlles, G. López and J. L. Bosch, "On The Use Of The Digital Elevation Model To Estimate The Solar Radiation In Areas Of Complex Topography", Meteorological Applications, vol. 13, no. 3, **(2007)**, pp. 279-287.
[14] X. P. Gu, S. J Yuan, L. Shi, W. M. Kang, Q. L. Miu and X. F. Qiu, "Study on distributed simulation of diffuse solar radiation over complex terrains based on DEM--Taking Guizhou plateau for example", Plateau Meteorology, vol. 28, no. 1, **(2009)**, pp. 143-150.
[15] S. J. Yuan, X. P. Gu and Q. L. Miao, "Distributed models of astronomical solar radiation over rugged terrains based on GIS", Journal of Mountain Science, vol. 25, no. 5, **(2007)**, pp. 577-583.
[16] X. P. Gu, S. J. Yuan, L. Shi, W. M. Kang, Q. L. Miu and X. F. Qiu, "Study on distributed simulation of diffuse solar radiation over complex terrains based on DEM--Taking Guizhou plateau for example", Plateau Meteorology, vol. 28, no. 1, **(2009)**, pp. 143-150.
[17] S. J. Yuan, Q. L. Miao, X. P. Gu and X. F. Qiu, "The elaborate distribution of direct solar radiation over rugged terrains in the Guizhou plateau", Journal of Natural Resources, vol. 24, no. 8, **(2009)**, pp. 1432-1439.
[18] X. P. Gu, S. J. Yuan, L. Shi, Q. L. Miu, W. M. Kang, X. F. Qiu and F. Z. Wang, "The elaborate spatial distribution of global solar radiation over complex terrains in Guizhou plateau", Journal of Mountain Science, vol. 28, no. 1, **(2010)**, pp. 96-102.
[19] K. H. Wang, M. J. Li, Y. Jiang and H. Li, "The spatial distribution of astronomical radiation under the rugged terrain in Shenzhen", Meteorology Journal of Inner Mongolia, vol. 3, **(2009)**, pp. 3-5.
[20] L. F. Zhu, Y. Z. Tian, T. X. Yun, Z. M. Fan, S. N. Ma and Y.A.Wang, "Simulation of solar radiation on ground surfaces based on 1km grid-cells", Transactions of the Chinese Society of Agricultural Engineering, vol. 21, no. 5, **(2005)**,pp. 16-19.
[21] P. M. Rich, R. Dubayah, W. A. Hetrick and S. C. Saving, "Using View shed Models to Calculate Intercepted Solar Radiation, Applications in Ecology", American Society for Photogrammetry and Remote Sensing Technical Papers **(1994)**, pp. 524–529.
[22] P. M. Rich and P. Fu, "Topoclimatic Habitat Models", Proceedings of the Fourth International Conference on Integrating GIS and Environmental Modeling,**(2000)**.
[23] P. Fu and P. A. Rich, "Geometric solar radiation model with applications in agriculture and forestry", Computers & Electronics in Agriculture, vol. 37, no. 2, **(2002)**, pp. 25-35.
[24] P. Fu and P. M. Rich, "The Solar Analyst 1.0 Manual. Helios Environmental Modeling Institute (HEMI), USA, **(2000)**.
[25] P. Fu and P. M. Rich, "Design and Implementation of the Solar Analyst: an ArcView Extension for Modeling Solar Radiation at Landscape Scales", Proceedings of the Nineteenth Annual ESRI User Conference, **(1999)**, San Diego, USA,

 

# Author

Xiaodan Mei* (1979--), Lecturer, PhD candidate, mainly engaged in the automatic map generalization, physical geography,3S technology and its application. E-mail：mxd2014ch@163.com.

Wenyi Fan (1965--), Ph.D., Professor. mainly engaged in forestry remote sensing, 3S technology and its application. fanwy@163.com.

Xuegang Mao (1981--), Ph.D., Lecturer. mainly engaged in forestry remote sensing, 3S technology and its application. maoxuegang@aliyun.com.